

12. B. D. Henshall and R. F. Cash, "Observations of the flow past a two-dimensional 4 per cent thick biconvex airfoil at high subsonic speed," Rep. Memo. Gr. Brit. Aeron. Res. Council., No. 3092, London (1958).
13. J. W. Miles, The Potential Theory of Unsteady Supersonic Flow, Cambridge University Press, Cambridge (1959).
14. Yu. A. Abramov, "Unsteady aperiodic motions of a bearing surface in a subsonic gas stream," in: Asymptotic Methods in the Theory of Unsteady Processes [in Russian], Nauka, Moscow (1971).

CALCULATION OF THE MOVEMENT OF A TWISTED FLOW OF A GAS SUSPENSION
ABOUT THE END OF A SEMI-INFINITE CYLINDER

I. Kh. Enikeev

UDC 532.529

This article examines the transverse movement of a twisted flow of a gas suspension about the end of a semi-infinite cylinder. The flow of the suspension is studied near the contact surface. The study is conducted within the framework of a three-velocity, three-temperature scheme describing the motion of interpenetrating continua. Questions relating to the formulation of the boundary conditions are also discussed. We determine the range of variation of the governing parameters within which reverse-circulating flow of the gas and particles takes place.

In most of the theoretical studies devoted either to the external flow of a gas suspension about a body or to the investigation of internal flows of disperse media, it is assumed particles which come into contact with a solid surface disappear from the flow [1-5]. Such a formulation of the problem is most appropriate for the case when the disperse phase consists of liquid drops or particles which form a thin film along the surface of the body after they come into contact with it.

If the disperse phase forms solid particles, the formulation of the boundary conditions becomes more complicated: it is necessary to introduce additional phases - a phase of particles reflected from the solid surface [6, 7] and a phase of particles moving randomly near the body in the flowing gas suspension [8].

1. Formulation of the Problem. We will examine the movement of a twisted flow of a gas suspension around a semi-infinite cylindrical end located within a contact surface which is coaxial with it (Fig. 1).

In accordance with [7], we introduce a fraction (phase) of incident particles (particles flying to the surface of the body in the flow) and a fraction of reflected particles (particles flying away from the surface, in the direction opposite the incident particles). As has already been noted, in the case of flow past blunt bodies, allowance for collisions between particles of different fractions makes it necessary to introduce an additional particle phase which moves randomly near the surface of the body in the gas suspension. Here, it is necessary to consider the velocity, pressure, and energy associated with the random motion resulting from collisions of particles of different fractions. Now the formulation of the problem is complicated to the extent that it cannot even be modeled numerically on a computer. Investigators have therefore found the range of determining parameters within which effects connected with randomization of the particles can be ignored. Thus, the estimates reported in [9] showed that randomization of the particles can be ignored when the mass content of particles in the incoming flow is on the order of 0.5-1. Within the framework of the proposed model, the equations describing the given problem have the form [7]

$$\frac{\partial \rho_1}{\partial t} + \operatorname{div} \rho_1 \mathbf{v}_1 = 0, \quad \frac{\partial \rho_i}{\partial t} + \operatorname{div} \rho_i \mathbf{v}_i = J_{ij} \quad (i \neq j; i, j = 2, 3),$$

$$\frac{\partial \rho_1 \mathbf{v}_1}{\partial t} + \nabla^h (\rho_1 \mathbf{v}_1 v_1^h) = -\nabla p - \mathbf{f}_{12} - \mathbf{f}_{13},$$

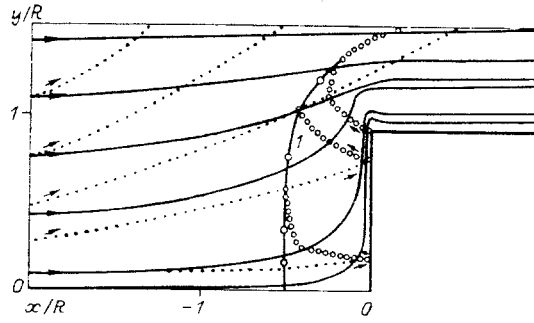


Fig. 1

$$\frac{\partial \rho_i \mathbf{v}_i}{\partial t} + \nabla^k (\rho_i v_i v_i^k) = \mathbf{f}_{i1} - \mathbf{f}_{ij} + J_{ij} \mathbf{v}_3,$$

$$\sum_{i=1}^3 \left[\frac{\partial \rho_i E_i}{\partial t} + \nabla^k (\rho_i E_i + \delta p) v_i^k \right] = 0, \quad \delta = \begin{cases} 0, & i = 2, 3, \\ 1, & i = 1, \end{cases} \quad (1.1)$$

$$\frac{\partial \rho_i e_i}{\partial t} + \nabla^k (\rho_i e_i v_i^k) = q_{1i} + J_{ij} e_3 + \frac{1}{2} \mathbf{f}_{ij} (\mathbf{v}_i - \mathbf{v}_j) + \frac{1}{2} J_{i,j} (\mathbf{v}_i - \mathbf{v}_j)^2,$$

$$E_i = e_i + \frac{1}{2} \mathbf{v}_i^2,$$

where the subscript $i \neq j$ ($i, j = 2, 3$) pertains to parameters of the incident and reflected particles, respectively; k is the summation index pertaining to the axes of the Cartesian coordinate system; ρ_i , \mathbf{v}_i , e_i , and E_i are the corrected density, velocity vector, and internal and total energies of the i -th phase; p is the pressure in the gas; \mathbf{f}_{ij} , q_{ij} are the friction vector and the rate of heat transfer between the gas and the particles; \mathbf{f}_{ij} , and $J_{i,j}$ are the vector of the effective interaction force and the rate of mass transfer between the second and third phases as a result of particle collision.

The equations of state of the phases are as follows:

$$p = \rho_1^0 (\gamma - 1) e_1, \quad e_1 = c_{V1} T_1, \quad e_2 = c_2 T_2, \quad e_3 = c_3 T_3.$$

Here, γ is the adiabatic exponent of the gas; $\rho_2^0 = \rho_3^0 = \text{const}$; c_{V1} , $c_2 = c_3$ are the isochoric heat capacity of the gas at constant volume and the heat capacity of the particles, respectively; T_i is the temperature of the phase; ρ_i^0 is the true density of the phase.

As in [7], the expressions for the rates of mechanical and thermal interaction between the phases will be represented as follows, with allowance for mass transfer between the incident and reflected particles as a result of collision

$$J_{32} = k^{(J)} \frac{\rho_2 \rho_3 |\mathbf{v}_2 - \mathbf{v}_3|}{\rho_2^0 d}, \quad \mathbf{f}_{32} = \frac{k^{(f)} \rho_2 \rho_3 (\mathbf{v}_2 - \mathbf{v}_3) |\mathbf{v}_2 - \mathbf{v}_3|}{\rho_2^0 d}$$

(d is particle diameter). The coefficients defining the interactions due to collisions of incident and reflected particles are taken equal to:

$$k^{(J)} = k^{(f)} = 0.1.$$

This value for $k^{(f)}$ agrees with the experimental data in [10] in relation to the hydraulics of polydisperse flows (air and particles of quartz sand) with relative phase velocities $\Delta v \approx 10$ m/sec.

2. Numerical Integration. The problem formulated in Part 1 was solved numerically by a modification of the coarse-particle method [11]. The essence of the modification - proposed in [11] - is the use of a difference scheme that is implicit with respect to time in the Eulerian stage of the process. Such an approach makes it possible to use the coarse-particle method to calculate flows with relatively small Mach numbers M_0 ($M_0 \lesssim 0.1$) when

$$\frac{\Delta \tau}{\Delta x} = 0.1, \quad \Delta \tau = \frac{\Delta t}{t_0}, \quad \Delta x = \frac{\Delta x}{R}, \quad t_0 = \frac{R}{U_0},$$

where R is a characteristic linear dimension of the problem (such as the radius of the end at $x = 0$); U_0 is the characteristic velocity (the velocity of the gas in the undisturbed flow).

As in the case of a two-phase model of motion in the Eulerian stage, intermediate values are calculated for only the gas phase. The parameters of the second and third phases remain constant at this stage, since the low volume concentration of the disperse phase means that there is no pressure gradient in the equations for the solid phase. The transfer of the mass, momentum, and energy of each phase across the boundary of the cells is calculated at the Lagrangian stage. In the final stage, conservation laws are used to find values for the parameters of all phases on the new time layer. Here, allowance is made for mechanical interaction between the phases f_{ij} ($i \neq j$; $i, j = 1, 2, 3$), the rate of mass transfer between the second and third phases J_{32} , and the flows of heat q_{12} , q_{13} from the gas to the incident and reflected particles, respectively. As in the case of a two-phase medium, the parameters of the solid phase are calculated first in the algorithm. The theoretical region had the form of a rectangle divided into 42 cells lengthwise and 22 cells in the height direction. The dimensionless distance step in the integration was $\Delta x = 0.082$, and the dimensionless time step in the integration was $\Delta \tau / \Delta x = 0.1$.

The boundary conditions for the gas and particles were as follows:

1. We used the conditions of an undisturbed flow without slip on the left boundary $x = -2$ (see Fig. 1) of the cylindrical region, on the side of the incoming two-phase flow:

$$v_1^x = v_2^x = U_0, v_1^y = v_2^y = 0, \rho_2 = \rho_{20}, p = p_0, T_1 = T_2 = T_0.$$

We also assumed that the gas and the particles were twisted in accordance with the rigid-body law, i.e.,

$$v_1^\varphi = v_2^\varphi = k_{\omega\infty}^R y / R$$

($k_{\omega\infty}^R$ is a coefficient expressing the twist of the disperse flow in the section $x = -2$).

2. On the lower boundary ($y = 0$) - considered to be the axis of symmetry of the end in the flow and located parallel to the velocity of the incoming flow U_0 - we took symmetry conditions for both the gas and the disperse particles.

3. We adopted the condition of impermeability on the upper [$y = (3/2)R$] contact surface for the gas and the condition of the absence of reflection for the particles. In other words, all of the particles that come into contact with this surface disappeared from the flow.

4. On the right ($x = 1$) open boundary of the region, we extrapolated the flow beyond the computed region; the derivatives of the velocities of the phases and pressures with respect to the normal were nearly equal to zero on this boundary.

5. We adopted the condition of impermeability $v_1^n = 0$ for the gas on the surface of the body, while for the disperse phase a boundary condition was needed only on the front surface (facing the incoming flow). Particles were absent from the rest of the body's surface. The following reflection condition was adopted for the particles on the front surface

$$v_3^n = -k^{(n)} v_2^n \quad (v_i^n = \mathbf{v}_i \cdot \mathbf{n}; \quad i = 2, 3), \quad \mathbf{v}_3 - v_3^{(n)} \mathbf{n} = k^{(\tau)} (\mathbf{v}_2 - v_2^{(n)} \mathbf{n}),$$

where $k^{(n)}, k^{(\tau)} \leq 1$ are the coefficient of restitution of normal velocity in impact and the coefficient of dynamic friction. The values of these coefficients depend on the properties and state of the colliding surfaces. We assumed that $k^{(n)} = k^{(\tau)} = 0.7$. Calculations were performed for different values of $k_{\omega\infty}^R$, $m_{20} = \rho_{20} / \rho_{10}^0$, $Stk = \rho_2^0 U_0 d^2 / 18\mu R$.

3. Description of the Results. Figure 1 shows the streamlines of the phases with the Stokes number $Stk = 0.1$, $k^{(J)} = k^{(f)} = 0.1$, $k^{(n)} = 0.7$, $k_{\omega\infty}^R = 0.1$, $M_0 = 0.08$, $m_{20} = 1$. The following notation is used here and in Fig. 2: the solid lines represent the streamlines of the gas phase, the points represent the streamlines of the incident particles, the circles denote the streamlines of the reflected particles, and curve 1 shows the envelope of the streamlines of the reflected particles (the separatrix). The calculations showed that the flow pattern is as follows. A region of high particle concentration, bounded by the separatrix, is formed ahead of the body. Reflected particles do not penetrate the incoming flow behind this region, which is thus the envelope of the reflected-particle streamlines. The normal velocity of the reflected particles is zero on the separatrix, and stagnation of the gas and incident particles causes reflected particles to build up and increase in concentration repeatedly. This buildup is limited by lateral removal of particles by the gas flowing over the cylindrical end and a $3 \rightarrow 2$ phase transition occurring as a result of collisions between incident and reflected particles. Reflected particles are thus able to enter the incoming flow. As can be seen in Fig. 3, the mass content of the disperse phase on the separatrix is approximately 10 times greater than the particle concentration in the incoming flow.

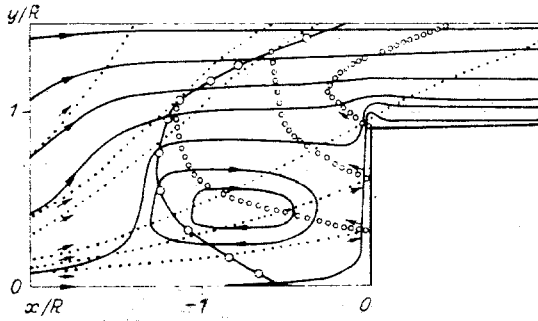


Fig. 2

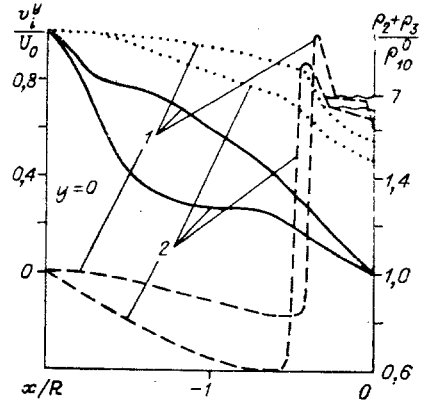


Fig. 3

However, the volume concentration $\alpha_3 = \rho_3/\rho_2^0 \approx 0.004$ ($\rho_2^0 = 2500 \text{ kg/m}^3$), which allows us to ignore the volume contents of the phases in Eqs. (1.1) throughout the flow region.

Figure 2 shows the streamlines of the phases for the same values of the determining parameters as in Fig. 1, but with $k_{\omega\infty}^R = 0.25$. The variants with increasing values of $k_{\omega\infty}^R$ shown in Figs. 1 and 2 illustrate that there are basically two different flow regimes. At $k_{\omega\infty}^R \leq 0.15$, nonseparated flow takes place about the semi-infinite cylinder. At $k_{\omega\infty}^R \geq 0.25$, a region of reverse-circulating motion of the gas is formed ahead of the end of the cylinder. Meanwhile, as can be seen from Figs. 1 and 2, the profile of the separatrix undergoes significant distortion. The separatrix has the form of a parabola whose branches are directed toward body. The vertex is located a distance on the order of R from the symmetry axis. It is seen that no substantial change in the profile of the separatrix takes place with a change in Stk or m_{20} . It is interesting to note that an increase in $k_{\omega\infty}^R$ is accompanied by a significant (by a factor of two or more) increase in the distance between the separatrix and the end of the cylinder. This is connected with the fact that at large $k_{\omega\infty}^R$ the reverse-circulating gas flow sharply reduces the dynamic head exerted on the reflected particles by the carrier phase. At the same time, there is also a decrease in the stagnating effect exerted on the reflected particles by the incident particles due to the decrease in their concentration in the wall region.

As was shown in [12], in the flow of an incompressible fluid past a blunt body in a cylindrical tube, the distributions of the axial u and tangential w components of velocity can be approximately obtained from the relations

$$\frac{u}{U_0} = 1 + 0,5 \left(\frac{R^2}{a^2} - 1 \right) \frac{kaJ_0(ky)}{J_1(ka)}; \quad (3.1)$$

$$\frac{w}{\Omega y} = 1 + \left(\frac{R^2}{a^2} - 1 \right) \frac{aJ_1(ky)}{yJ_1(ka)}, \quad \Omega = \frac{k_{\omega\infty}^R U_0}{R}, \quad k = \frac{2k_{\omega\infty}^R}{R}, \quad (3.2)$$

where $J_0(ky)$ and $J_1(ky)$ are Bessel functions of the first kind; a is the height of the body in the flow. Downstream on the tube axis

$$\left(\frac{u}{U_0} \right)_{y=0} = \left(\frac{w}{\Omega y} \right)_{y=0} = 1 + 0,5 \left(\frac{R^2}{a^2} - 1 \right) \frac{ka}{J_1(ka)}.$$

It follows from (3.1)-(3.2) that mainly negative values of u are seen on the tube axis at $ak \geq 2.4$. A qualitative explanation of this is that expansion of the flow is accompanied by a redistribution of pressure in the liquid, which in turn leads to formation of the reverse axial flow. This is illustrated in Fig. 3, where the solid lines and the points represent the velocity profiles of the gas and incident particles and the dashed lines show the distribution of the overall density of the disperse phase. Curves 1 and 2 correspond to $k_{\omega\infty}^R = 0.1, 0.25$. The calculations were performed with the same values of the determining parameters as in Figs. 1 and 2. Figure 3 shows that an increase in $k_{\omega\infty}^R$ in the axial region is accompanied by a substantial reduction in gas velocity due to the presence of the reverse-circulating motion. This in turn leads to a decrease in the velocity of the incident particles. Collisions of incident and reflected particles result in an even greater decrease in the velocity of the incident particles behind the separatrix. It is evident from Fig. 3 that the concentration profile of the disperse phase is of a distinctly nonmonotonic nature, which is connected with the existence of a centrifugal force that moves particles out of the axial

region and thus lowers their concentration in the latter. As was shown in [7], there is an abrupt increase in the concentration of reflected particles on the separatrix, which leads to the formation of a narrow zone in which the concentration of the disperse phase undergoes a significant increase. The concentration of this phase decreases as the end of the cylinder is approached but remains appreciably greater than in the incoming flow (see Fig. 3).

LITERATURE CITED

1. Yu. P. Golovachev and A. A. Shmidt, "Movement of a supersonic flow of a dust-laden gas past a blunt body," *Izv. Akad. Nauk SSSR, Mekh. Zhidk. Gaza*, No. 3 (1982).
2. Yu. M. Davydov and R. I. Nigmatulin, "Calculation of the movement of heterogeneous flows of a gas with drops or particles outside blunt bodies," *Dokl. Akad. Nauk SSSR*, 269, No. 1 (1981).
3. A. D. Rychkov, *Mathematical Modeling of Gas-Dynamic Processes in Channels and Nozzles* [in Russian], Nauka, Novosibirsk (1988).
4. U. G. Pirumov and V. N. Suvorova, "Numerical solution of an inverse problem in the theory of nozzles for a two-phase mixture of gas and particles," *Izv. Akad. Nauk SSSR, Mekh. Zhidk. Gaza*, No. 4 (1986).
5. V. I. Kopchenov, "Solution of an inverse problem concerning the flow of a two-phase mixture of gas and foreign solid or liquid particles in a de Laval nozzle," *Prikl. Mekh. Tekh. Fiz.*, No. 6 (1975).
6. N. N. Yanenko, A. P. Alkhimov, N. I. Nesterovich, et al., "Change in the wave structure during the movement of a two-phase supersonic flow past bodies," *Dokl. Akad. Nauk SSSR*, 260, No. 4 (1981).
7. R. I. Nigmatulin, *Dynamics of Multiphase Media* [in Russian], Vol. 1, Nauka, Moscow (1987).
8. S. K. Matveev, "Model of a gas of solid particles with allowance for inelastic collisions," *Izv. Akad. Nauk SSSR, Mekh. Zhidk. Gaza*, No. 6 (1983).
9. I. M. Vasenin, V. A. Arkhipov, V. G. Butov, et al., *Gas Dynamics of Two-Phase Flows in Nozzles* [in Russian], TGU, Tomsk (1986).
10. R. L. Babukha and A. A. Shraiber, *Interaction of Particles of a Polydisperse Material in Two-Phase Flows* [in Russian], Naukova Dumka, Kiev (1972).
11. I. Kh. Enikeev, O. F. Kuznetsova, V. A. Polyanskii, and E. F. Shurgal'skii, "Mathematical modeling of twisted two-phase flows by a modification of the coarse-particle method," *Zh. Vychisl. Mat. Mat. Fiz.*, 28, No. 1 (1988).
12. J. Batchelor, *Introduction to Fluid Dynamics* [Russian translation], Mir, Moscow (1973).

INTERACTION OF A SHOCK WAVE WITH A BOUNDARY LAYER

V. I. Bergel'son, Yu. N. Kiselev,
V. A. Klumov,* I. V. Nemchinov,
T. I. Orlova, V. B. Rozhdestvenskii,
and V. M. Khazins

UDC 533.6.011

The propagation of a high-intensity shock wave in a gas along a solid surface is accompanied by distortion of the shock front — a wedge-shaped precursor which becomes larger over time is formed near the surface [1]. One possible reason for this phenomenon is the formation of a heated layer of gas or erosive vapor near the surface [2]. Analogous to this phenomenon is the thermal-layer effect discovered by G. I. Taganov [3, 4]. The restructuring that the flow undergoes when a thermal (low-density) layer precedes the shock front is of a global nature, since it occurs in a region much larger than the thickness of the perturbing layer. It was subsequently noted [5] that a precursor is formed when the surface of the wall vaporizes. Detailed spectral measurements made in [6, 7] showed that the given phenomenon does indeed begin to unfold in a thin vaporous boundary layer heated by radiation. At the same

*Deceased.

Moscow. Translated from *Prikladnaya Mekhanika i Tekhnicheskaya Fizika*, No. 3, pp. 32-40, May-June, 1993. Original article submitted January 9, 1990; revision submitted May 14, 1992.